A Two-Step Deep Learning Approach for Abdominal Organ Segmentation

Jianwei Gao[0000−0002−6358−4117], Juan Xu, Honggao Fei, and Dazhu Liang

Digital Health China Technologies Co., LTD, Beijing, China
{gaojw,xujuan,feihg}@dchealth.com

Abstract. Accurate delineation and analysis of anatomical structures within medical images are essential in various clinical applications, with medical image segmentation playing a key role. In the context of abdominal imaging, the precise segmentation of organs like the liver, spleen, and kidneys holds significant importance for tasks such as diagnosis, treatment planning, and surgical interventions. However, achieving precise and efficient segmentation of abdominal organs poses significant challenges due to the variability in organ shape, size, and appearance across different patients and imaging modalities. The MICCAI FLARE23 segmentation paper presents a solution to the challenging problem of segmenting 13 organs and tumor from CT scans, provided 2200 CT scans with partial labels and 1800 CT scans without labels, while balancing model performance and resource consumption. To address these challenges, the paper proposes a two-step segmentation approach that combines organ segmentation and tumor segmentation, which are both accomplished with nnU-Net model. We also crop some top and bottom slices for faster process.

Keywords: Abdominal organ segmentation · Supervised Learning · nnUnet.

1 Introduction

Medical image segmentation plays a pivotal role in various clinical applications, enabling the accurate delineation and analysis of anatomical structures within medical images. However, achieving precise and efficient segmentation of abdominal organs poses significant challenges, because it typically requires a large amount of labeled data to train an accurate model, while manually annotating organs from CT scans is a time-consuming and labor-intensive process, furthermore, abdominal organs may have complex morphological structures and heterogeneous lesions, which segmentation a more difficult task.

In recent years, deep learning became the mainstream method for medical image analysis, demonstrating remarkable capabilities in automated organ segmentation tasks. [9] Specifically, the nnU-Net model [7] has emerged as a powerful framework for achieving state-of-the-art results in medical image segmentation. nnU-Net combines the strengths of the U-Net architecture with advancements in neural network design and training strategies, allowing for improved accuracy

and robustness. Semi-supervised segmentation [15] is a type of segmentation where the training set consists of both labeled and unlabeled data. The goal is to assign pseudo-labels to the pixels of unlabeled images. This approach is useful when obtaining labeled data is expensive or time-consuming, which is perfect for this challenge.

Because there are no full 14 classes labeled data but 13 classes organ segmentation labeled data, in this paper,we break it down into two tasks: organ segmentation and tumour segmentation. Therefor, we propose an approach which involved training two nnUnet model with labeled data, which are used to segment organs and tumours respectively. A post-process is used to merge two Deep Learning results when inferencing.

2   Method

2.1   Preprocessing

We use several pre-processing strategies as follows.

- Data choose and preprocessing
  We choose train data with full 13 organ label and data with tumor label, thus get 222 data for organ segment and 735 for tumor segment. then we split them by 8:2 ratio for train and validation.
- Cropping strategy
  We use the CT scans as the data source to generate the bounding box of foreground, and then crop only the foreground object of the images.
- Resampling method for anisotropic data
  We resample the original data to unify the voxel spacing into $[1.0, 1.0, 1.0]$.
- Intensity normalization method
  We collect intensity values from the foreground classes (all but the background and ignore) from all training cases, compute the mean, standard deviation as well as the 0.5 and 99.5 percentile of the values. Then clip to the percentiles, followed by subtraction of the mean and division with the standard deviation. The normalization that is applied is the same for each training case (for this input channel).

2.2   Deep Network

Figure 1 illustrates the applied 3D nnU-Net [7], where a 3D U-Net architecture is adopted. We use the leaky ReLU function with a negative slope of 0.01 as the activation function. Our first 3D nnU-Net has 14 out channels, corresponding to the background and 13 organs, while our second 3D nnU-Net has 2 out channels, corresponding to the background and the tumor. In this case, only data with 13 organ label and data with tumor label are used, the others is abandon.Unlabeled images were not used.

We use the sum of Dice loss (after applying a softmax function) and Cross Entropy Loss as the loss function, because it's a popular choice for loss fuction and have been proven to be robust in various medical image segmentation tasks.
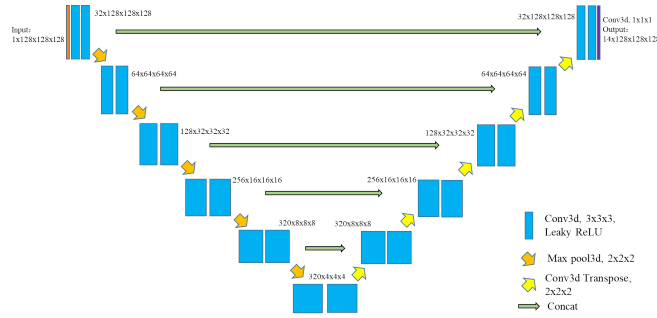
Fig. 1. Our 3D U-Net architecture

When predicting a single image with the trained segmentation model, we first resample it to a voxel spacing of [1.0, 1.0, 1.0], as we did during training, and try to predict. In order to improving inference speed and reducing resource consumption, we crop top and bottom slices of the data in predicting, only keep only the middle 50 slices.

2.3   Post-processing

During model prediction, we select the label (from 0 to 13) corresponding to the largest of the 13 outputs for each voxel, after that, we combine predictions of two model to get the final result. when one pixel is both predicted as tumor and organ, it will be considered as tumor. finally, we add full 0 array as top and bottom slices

3   Experiments

3.1   Dataset and evaluation measures

The FLARE 2023 challenge is an extension of the FLARE 2021-2022 [11][12], aiming to aim to promote the development of foundation models in abdominal disease analysis. The segmentation targets cover 13 organs and various abdominal lesions. The training dataset is curated from more than 30 medical centers under the license permission, including TCIA [2], LiTS [1], MSD [14], KiTS [5,6], autoPET [4,3], TotalSegmentator [16], and AbdomenCT-1K [13]. The training set includes 4000 abdomen CT scans where 2200 CT scans with partial labels and 1800 CT scans without labels. The validation and testing sets include 100 and 400 CT scans, respectively, which cover various abdominal cancer types, such as liver cancer, kidney cancer, pancreas cancer, colon cancer, gastric cancer, and so on. The organ annotation process used ITK-SNAP [17], nnU-Net [8], and MedSAM [10].

The evaluation metrics encompass two accuracy measures—Dice Similarity Coefficient (DSC) and Normalized Surface Dice (NSD)—alongside two efficiency

measures—running time and area under the GPU memory-time curve. These metrics collectively contribute to the ranking computation. Furthermore, the running time and GPU memory consumption are considered within tolerances of 15 seconds and 4 GB, respectively.

3.2 Implementation details

Environment settings The development environments and requirements are presented in Table 1.

Table 1. Development environments and requirements.

Windows/Ubuntu version	Ubuntu 20.04.4 LTS
CPU	Intel(R) Xeon(R) Gold 5218R CPU @ 2.10GHz
RAM	128G
GPU (number and type)	NVIDIA Tesla T4 (16G)
CUDA version	11.6
Programming language	Python 3.9
Deep learning framework	Pytorch (Torch 1.13.1, torchvision 0.14.1)
Specific dependencies	numpy 1.25.2, SimpleITK 2.2.1, nnunetv2 2.1 nibabel 5.1.0

Training protocols As described below.

Random flipping strategy (only for initial training stage): each image has a 20% probability of flipping along the x-axis and a 20% probability of flipping along the y-axis.

Random Gaussian smooth (only for initial training stage): each image has a 10% probability of being Gaussian smoothed with sigma in (0.5, 1.15) for every spatial dimension.

Random Gaussian noise (only for initial training stage): each image has a 20% probability of being added with Gaussian noise with mean in (0, 0.5) and standard deviation in (0, 1).

Random intensity change (only for initial training stage): each image has a 10% probability of changing intensity with gamma in (0.5, 2.5).

Random intensity shift (only for initial training stage): each image has a 10% probability of shifting intensity with offsets in (0, 0.3).

Patch sampling strategy: 2 patches of size $[128, 128, 128]$ are randomly cropped from each image. The center of each patch has 50% probability in the foreground and 50% probability in the background.

As described above,only data with 13 organ label and data with tumor label are used, the others is abandon. Unlabeled images were not used.

Some details of the initial training stage and the fine-tuning stage are shown in Table 2 and Table 3 respectively.

Table 2. Training protocols (initial training stage).

Network initialization	"he" normal initialization
Batch size	2
Patch size	128×128×128
Total epochs	1000
Optimizer	Adam
Initial learning rate (lr)	0.0001
Lr decay schedule	initial learning rate$\times(1 - epoch/500)^{0.9}$
Training time	20 hours
Loss function	the sum of dice loss and cross entropy loss
Number of model parameters	31.42M

Table 3. Training protocols (fine-tuning stage).

Network initialization	model after initial training
Batch size	2
Patch size	128×128×128
Total epochs	40
Optimizer	Adam
Initial learning rate (lr)	0.00005
Lr decay schedule	initial learning rate$\times(1 - epoch/500)^{0.9}$
Training time	39 hours
Loss function	the sum of dice loss and cross entropy loss
Number of model parameters	31.42M

4   Results and discussion

4.1   Quantitative results on validation set

DSC and NSD results on validation set are shown in Table 4. It can be seen from the table that Aorta and LK have best proformance, while others has worst proformance.A possible reason of it is that Aorta and LK is larger organ and more likely in the center,therefor not be croped by preprocessing.

Table 4. Results on validation set.

Target	Public Validation		Online Validation		Testing	
	DSC(%)	NSD(%)	DSC(%)	NSD(%)	DSC(%)	NSD (%)
Liver	0.600± 0.600	0.000± 0.000	5.500	4.400		
RK	1.500± 1.500	1.110± 1.110	5.500	8.900		
Spleen	0.000± 0.000	0.000± 0.000	10.000	10.000		
Pancreas	0.440± 0.440	0.540± 0.540	5.100	7.500		
Aorta	8.860± 8.860	9.570± 9.570	6.870	7.460		
IVC	0.980± 0.980	0.820± 0.820	14.500	14.000		
RAG	4.000± 4.000	4.000± 4.000	2.000	2.000		
LAG	2.000± 2.000	2.000± 2.000	1.000	1.000		
Gallbladder	8.000± 8.000	8.000± 8.000	10.000	10.000		
Esophagus	0.000± 0.000	0.000± 0.000	0.0000	0.0000		
Stomach	0.000± 0.000	0.000± 0.000	0.0000	0.0000		
Duodenum	5.500± 5.500	9.400± 9.400	0.280	0.470		
LK	11.930± 11.930	11.480± 11.480	12.210	11.090		
Tumor	0.000± 0.000	0.000± 0.000	0.000	0.000		

Table 5. Quantitative evaluation of segmentation efficiency in terms of the running them and GPU memory consumption. Total GPU denotes the area under GPU Memory-Time curve.

Case ID	Image Size	Running Time (s)	Max GPU (MB)	Total GPU (MB)
0001	(512, 512, 55)	133.13	3746	30428
0051	(512, 512, 100)	143.65	3806	14327
0017	(512, 512, 150)	121.93	3590	24825
0019	(512, 512, 215)	85.79	3323	14863
0099	(512, 512, 334)	73.7	3374	11619
0063	(512, 512, 448)	72.57	3370	10082
0048	(512, 512, 499)	70.87	3316	10466
0029	(512, 512, 554)	74.38	3382	11035

4.2   Qualitative results on validation set

Two examples of good segmentation are shown in Figure 2 and two examples of bad segmentation are shown in Figure 3. Visualization is achieved with ITK-SNAP [18] version 3.6.0.

From the perspective of images, some potential reasons for the bad-segmentation cases are listed below.

(1) The size of the case is very large, so we have to reduce the size of the case by cutting top and bottom slice to process it in 60 second.

(2) The case is not clear, distorted, or skewed.

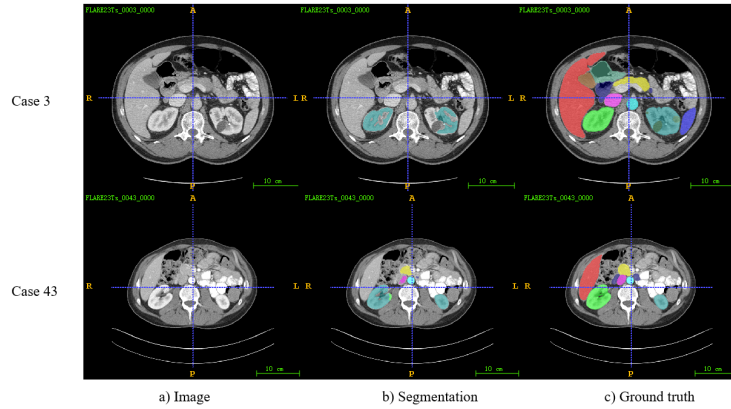(3) There are rare structures in the case that are not in the training set.

Fig. 2. Good segmentation examples

4.3   Segmentation efficiency results on validation set

Table 5 show the efficiency results on 8 validation sets.Due to the crop of top and bottom slices, the data which has larger thrid-dimension also have fast running times.

4.4   Results on final testing set

4.5   Limitation and future work

In terms of model accuracy, first, we does not use pseudo-labels for unlabeled image at present. In the future, we are going to use pseudo-labels for unlabeled image. Second, we consider using some post-processing methods, such as largest connected component extraction, hole filling, open operation and closed operation, which are not used at present.

to reduce the time consumption, we simply cut top and bottom slices, which caused a large loss of accuracy. To deal with it, we consider using some optimization methods to improve the running speed of the model in the future.
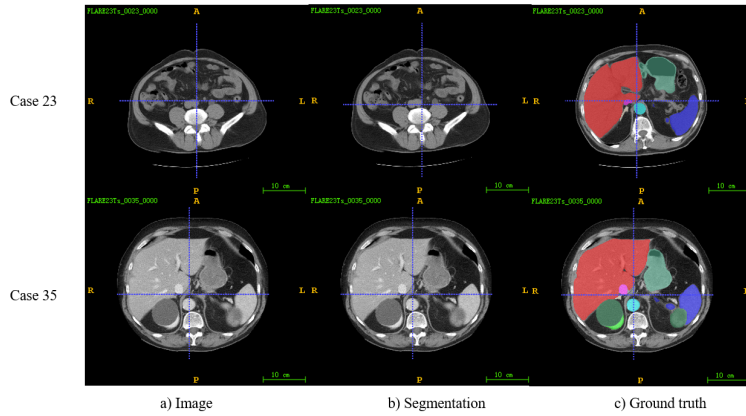
a) Image   b) Segmentation   c) Ground truth

Fig. 3. Bad segmentation examples

5   Conclusion

In this paper, we have explored the application of the nnU-Net model for Flare23 abdominal organ segmentation. Due to the limitation of time, we could not Leverage the power of deep learning and the architectural advancements of nnU-Net, but we will explore better deep learning methods in the future.

Acknowledgements The authors of this paper declare that the segmentation method they implemented for participation in the FLARE 2023 challenge has not used any pre-trained models nor additional datasets other than those provided by the organizers. The proposed solution is fully automatic without any manual intervention.

References

1. Bilic, P., Christ, P., Li, H.B., Vorontsov, E., Ben-Cohen, A., Kaissis, G., Szeskin, A., Jacobs, C., Mamani, G.E.H., Chartrand, G., Lohöfer, F., Holch, J.W., Sommer, W., Hofmann, F., Hostettler, A., Lev-Cohain, N., Drozdzal, M., Amitai, M.M., Vivanti, R., Sosna, J., Ezhov, I., Sekuboyina, A., Navarro, F., Kofler, F., Paetzold, J.C., Shit, S., Hu, X., Lipková, J., Rempfler, M., Piraud, M., Kirschke, J., Wiestler, B., Zhang, Z., Hülsemeyer, C., Beetz, M., Ettlinger, F., Antonelli, M., Bae, W., Bellver, M., Bi, L., Chen, H., Chlebus, G., Dam, E.B., Dou, Q., Fu, C.W., Georgescu, B., i Nieto, X.G., Gruen, F., Han, X., Heng, P.A., Hesser, J., Moltz, J.H., Igel, C., Isensee, F., Jäger, P., Jia, F., Kaluva, K.C., Khened, M., Kim, I., Kim, J.H., Kim, S., Kohl, S., Konopczynski, T., Kori, A., Krishnamurthi, G., Li, F., Li, H., Li, J., Li, X., Lowengrub, J., Ma, J., Maier-Hein, K., Maninis, K.K., Meine, H., Merhof, D., Pai, A., Perslev, M., Petersen, J., Pont-Tuset, J., Qi, J., Qi, X., Rippel, O., Roth, K., Sarasua, I., Schenk, A., Shen, Z., Torres, J., Wachinger, C., Wang, C., Weninger, L., Wu, J., Xu, D., Yang, X., Yu, S.C.H., Yuan, Y., Yue, M., Zhang,

L., Cardoso, J., Bakas, S., Braren, R., Heinemann, V., Pal, C., Tang, A., Kadoury, S., Soler, L., van Ginneken, B., Greenspan, H., Joskowicz, L., Menze, B.: The liver tumor segmentation benchmark (lits). Medical Image Analysis **84**, 102680 (2023) 3

2. Clark, K., Vendt, B., Smith, K., Freymann, J., Kirby, J., Koppel, P., Moore, S., Phillips, S., Maffitt, D., Pringle, M., Tarbox, L., Prior, F.: The cancer imaging archive (tcia): maintaining and operating a public information repository. Journal of Digital Imaging **26**(6), 1045–1057 (2013) 3

3. Gatidis, S., Früh, M., Fabritius, M., Gu, S., Nikolaou, K., La Fougère, C., Ye, J., He, J., Peng, Y., Bi, L., et al.: The autopet challenge: Towards fully automated lesion segmentation in oncologic pet/ct imaging. preprint at Research Square (Nature Portfolio) (2023). https://doi.org/https://doi.org/10.21203/rs.3.rs-2572595/v1 3

4. Gatidis, S., Hepp, T., Früh, M., La Fougère, C., Nikolaou, K., Pfannenberg, C., Schölkopf, B., Küstner, T., Cyran, C., Rubin, D.: A whole-body fdg-pet/ct dataset with manually annotated tumor lesions. Scientific Data **9**(1), 601 (2022) 3

5. Heller, N., Isensee, F., Maier-Hein, K.H., Hou, X., Xie, C., Li, F., Nan, Y., Mu, G., Lin, Z., Han, M., Yao, G., Gao, Y., Zhang, Y., Wang, Y., Hou, F., Yang, J., Xiong, G., Tian, J., Zhong, C., Ma, J., Rickman, J., Dean, J., Stai, B., Tejpaul, R., Oestreich, M., Blake, P., Kaluzniak, H., Raza, S., Rosenberg, J., Moore, K., Walczak, E., Rengel, Z., Edgerton, Z., Vasdev, R., Peterson, M., McSweeney, S., Peterson, S., Kalapara, A., Sathianathen, N., Papanikolopoulos, N., Weight, C.: The state of the art in kidney and kidney tumor segmentation in contrast-enhanced ct imaging: Results of the kits19 challenge. Medical Image Analysis **67**, 101821 (2021) 3

6. Heller, N., McSweeney, S., Peterson, M.T., Peterson, S., Rickman, J., Stai, B., Tejpaul, R., Oestreich, M., Blake, P., Rosenberg, J., et al.: An international challenge to use artificial intelligence to define the state-of-the-art in kidney and kidney tumor segmentation in ct imaging. American Society of Clinical Oncology **38**(6), 626–626 (2020) 3

7. Isensee, F., Jaeger, P.F., Kohl, S.A., Petersen, J., Maier-Hein, K.H.: nnu-net: a self-configuring method for deep learning-based biomedical image segmentation. Nature Methods **18**(2), 203–211 (2021) 1, 2

8. Isensee, F., Jaeger, P.F., Kohl, S.A., Petersen, J., Maier-Hein, K.H.: nnu-net: a self-configuring method for deep learning-based biomedical image segmentation. Nature Methods **18**(2), 203–211 (2021) 3

9. Kart, T., Fischer, M., Winzeck, S., Glocker, B., Bai, W., Bülow, R., Emmel, C., Friedrich, L., Kauczor, H.U., et al.: Automated imaging-based abdominal organ segmentation and quality control in 20,000 participants of the uk biobank and german national cohort studies. Scientific Reports (2022) 1

10. Ma, J., Wang, B.: Segment anything in medical images. arXiv preprint arXiv:2304.12306 (2023) 3

11. Ma, J., Zhang, Y., Gu, S., An, X., Wang, Z., Ge, C., Wang, C., Zhang, F., Wang, Y., Xu, Y., Gou, S., Thaler, F., Payer, C., Štern, D., Henderson, E.G., McSweeney, D.M., Green, A., Jackson, P., McIntosh, L., Nguyen, Q.C., Qayyum, A., Conze, P.H., Huang, Z., Zhou, Z., Fan, D.P., Xiong, H., Dong, G., Zhu, Q., He, J., Yang, X.: Fast and low-gpu-memory abdomen ct organ segmentation: The flare challenge. Medical Image Analysis **82**, 102616 (2022) 3

12. Ma, J., Zhang, Y., Gu, S., Ge, C., Ma, S., Young, A., Zhu, C., Meng, K., Yang, X., Huang, Z., Zhang, F., Liu, W., Pan, Y., Huang, S., Wang, J., Sun, M., Xu, W., Jia,

D., Choi, J.W., Alves, N., de Wilde, B., Koehler, G., Wu, Y., Wiesenfarth, M., Zhu, Q., Dong, G., He, J., the FLARE Challenge Consortium, Wang, B.: Unleashing the strengths of unlabeled data in pan-cancer abdominal organ quantification: the flare22 challenge. arXiv preprint arXiv:2308.05862 (2023) 3

13. Ma, J., Zhang, Y., Gu, S., Zhu, C., Ge, C., Zhang, Y., An, X., Wang, C., Wang, Q., Liu, X., Cao, S., Zhang, Q., Liu, S., Wang, Y., Li, Y., He, J., Yang, X.: Abdomenct-1k: Is abdominal organ segmentation a solved problem? IEEE Transactions on Pattern Analysis and Machine Intelligence **44**(10), 6695–6714 (2022) 3

14. Simpson, A.L., Antonelli, M., Bakas, S., Bilello, M., Farahani, K., van Ginneken, B., Kopp-Schneider, A., Landman, B.A., Litjens, G., Menze, B., Ronneberger, O., Summers, R.M., Bilic, P., Christ, P.F., Do, R.K.G., Gollub, M., Golia-Pernicka, J., Heckers, S.H., Jarnagin, W.R., McHugo, M.K., Napel, S., Vorontsov, E., Maier-Hein, L., Cardoso, M.J.: A large annotated medical image dataset for the development and evaluation of segmentation algorithms. arXiv preprint arXiv:1902.09063 (2019) 3

15. Wang, Y., Wang, H., Shen, Y., Fei, J., Li, W., Jin, G., Wu, L., Zhao, R., Le, X.: Semi-supervised semantic segmentation using unreliable pseudo-labels (2022) 2

16. Wasserthal, J., Breit, H.C., Meyer, M.T., Pradella, M., Hinck, D., Sauter, A.W., Heye, T., Boll, D.T., Cyriac, J., Yang, S., Bach, M., Segeroth, M.: Totalsegmentator: Robust segmentation of 104 anatomic structures in ct images. Radiology: Artificial Intelligence **5**(5), e230024 (2023) 3

17. Yushkevich, P.A., Gao, Y., Gerig, G.: Itk-snap: An interactive tool for semi-automatic segmentation of multi-modality biomedical images. In: Annual International Conference of the IEEE Engineering in Medicine and Biology Society. pp. 3342–3345 (2016) 3

18. Yushkevich, P.A., Piven, J., Cody Hazlett, H., Gimpel Smith, R., Ho, S., Gee, J.C., Gerig, G.: User-guided 3D active contour segmentation of anatomical structures: Significantly improved efficiency and reliability. Neuroimage **31**(3), 1116–1128 (2006) 7

Table 6. Checklist Table. Please fill out this checklist table in the answer column.

Requirements	Answer
A meaningful title	Yes
The number of authors (≤6)	4
Author affiliations and ORCID	Yes
Corresponding author email is presented	No
Validation scores are presented in the abstract	No
Introduction includes at least three parts: background, related work, and motivation	Yes
A pipeline/network figure is provided	Figure 1
Pre-processing	Page 2
Strategies to use the partial label	Page 2
Strategies to use the unlabeled images.	Page 2
Strategies to improve model inference	Page 3
Post-processing	Page 3
Dataset and evaluation metric section is presented	Page 3
Environment setting table is provided	Table 1
Training protocol table is provided	Table 2
Ablation study	Page 7
Efficiency evaluation results are provided	Table 5
Visualized segmentation example is provided	Figure 2/3
Limitation and future work are presented	Yes
Reference format is consistent.	Yes